

Smectic A liquid crystal configurations with interface defects

M. Carme Calderer*, Chun Liu and Karl Voss

*Department of Mathematics and Center for Materials Physics, Penn State University, University Park,
PA 16802, U.S.A.*

Communicated by G. C. Hsiao

SUMMARY

We study planar energy minimizing configurations of smectic A liquid crystal materials and classify the corresponding defect structures. We investigate focal conic configurations in wedge, non-parallel plates, funnel-shaped domains, and non-concentric annuli. The application of the *stability condition* for focal conics is relevant to the specification of the location of the interfacial defects. Self-similar structures are discussed for a class of solutions with the same bulk energy. We propose surface energies terms to serve as selection mechanisms of particular self-similar configurations. We also show how the modelling of chevron texture naturally arises in the present framework. Copyright © 2001 John Wiley & Sons, Ltd.

1. INTRODUCTION

This article discusses equilibrium planar layer configurations of smectic A liquid crystals confined in a domain determined by two plates (parallel as well as non-parallel) and two circles (concentric as well as non-concentric). We investigate the defect structures of energy minimizing configurations according to the shape of the domain and the boundary conditions on the fields.

The solutions that we construct illustrate the types of defect structures that occur in the smectic A phase of a liquid crystal, namely, *disclinations*, *dislocations* and *focal conics*. Whereas the latter corresponds to a pattern over the material domain, the other two are local and may exhibit features of either the nematic or the isotropic phase. We consider, both, *polar* and *non-polar* smectic A materials as described by the corresponding free energy functions. One of the main issues of the present article is to investigate how the shape of the domain, the boundary conditions on the fields and the constraint of prescribed layer spacing determine the wealth of focal conic structures and defect interfaces encountered in the smectic A liquid crystal phase.

*Correspondence to: M. Carme Calderer: Department of Mathematics and Center for Materials Physics, Penn State University, University Park, PA 16802, U.S.A.

Contract/grant sponsor: National Science Foundation; Contract/grant number: DMS-9704714

One of the most interesting phenomena concerning smectic A liquid crystals is the occurrence of the focal conic structure. Such a structure is a consequence of the property of equal layer spacing that characterizes the smectic A phase. The focal conic structure was first discovered by Friedel [1] and described as *texture à eventails* indicating the fanning appearance of the pattern. Among the wealth of studies of focal conic structures, we mention works by Kléman [2], Boltenhagen *et al.* [3], Kralj and Zumer [4], Ouchi *et al.* [5], that refer to experiments in a variety of geometrical settings.

Recently by using the method of the Ginzburg–Landau approximation, Kinderlehrer and Liu illustrated that, in two-space dimensions [6], the focal conic structure can be derived directly from the condition $\nabla \times \mathbf{n} = 0$. Moreover, they show that the energy density has the form of a distance function, resulting in (locally) planar and circular layers shapes of the energy minimizing configurations. In the previous article [7], we analysed layer configurations corresponding to energy minimizers in a disk. Works by Garcia and E [8], by Collings [21] and by Stewart *et al.* [9] deal with related modelling aspects of the smectic A phase.

Using the *stability condition* for focal conics introduced in Reference [6], we construct defect configurations for wedge, non-parallel plates, funnel domains, non-concentric annuli, and non-convex polygons. The stability condition establishes that the layers must be equidistant on both sides of the defect interface. It turns out to be a local characterization of conic sections (quadratic curves).

The understanding of solution structures in such domains provides valuable information for applications of smectic materials in the manufacturing of display devices [10, Chapters 1–4].

De Gennes proposed a free energy density reminiscent of the Landau theory of superconductivity with the aim of capturing relevant aspects of the smectic A behaviour [11, p.510]. The quadratic gradient terms of the density fields in that energy play the role of penalizing inhomogeneities. The tendency of \mathbf{n} to be perpendicular to the layers is formulated as an energy constraint. Both, *polar* and *non-polar* liquid crystals are encountered in nature as well as synthesized in the laboratory. Within the mathematical framework, the non-polar property corresponds to the invariance of the free energy density under the transformation of \mathbf{n} to $-\mathbf{n}$. We point out that the free energy proposed by de Gennes corresponds to polar smectic A configurations. In Reference [12], Calderer and Palfy-Muhoray proposed a free energy which may be appropriate to model non-polar smectic A behaviour. In this paper we discuss both types of phenomena, as described by the two different free energy density functions.

The models are presented and discussed in Section 2. In Section 3, the governing equations are derived in the planar layer case, for both polar and non-polar models. We study several limiting solutions, according to prescribed boundary conditions, in order to classify and distinguish among different types of defects.

Focal conic interfaces are discussed in Section 4. The newly constructed solutions have a defect interface, either with the shape of an ellipse, a hyperbola, or a parabola. In Section 5, the planar layer configuration is viewed as the limit of the circular layer case, with defect interfaces being straight lines. Applications to the study of defect configurations in wedge, non-parallel plates, funnel domains, non-concentric annuli, and non-convex polygons follow. The resulting configurations are non-unique, and self-similarity of solutions may occur. According to the model that we analyse, self-similar solutions have the same bulk energy. We give examples of surfaces energy terms that are capable of selecting unique solutions.

2. BASIC MODELS AND ENERGIES

In the absence of flow, a smectic A phase is fully characterized by the director field \mathbf{n} , with $\mathbf{n} = 1$, the density modulation ρ , and the phase ϕ . We let $\Psi = \rho e^{i\phi}$. The level sets of ϕ represent the layers. The field, ρ , plays a regularizing role in the model; the vanishing of such a field at a point indicates that the material exhibits nematic behaviour at that point. Often, this is referred to as a nematic (or isotropic) defect.

The smectic layer structure must be locally meaningful for all of the configurations described in this paper. Specifically, level surfaces, $\phi(\mathbf{r}) = \lambda$, $\lambda \in \mathbb{R}$, define a smectic A layer field in the neighbourhood of a point, $\mathbf{r}_0 \in \Omega$, provided that ϕ is continuously differentiable at \mathbf{r}_0 and

$$\nabla\phi(\mathbf{r}_0) = q\mathbf{n}, \quad |\mathbf{n}| = 1 \tag{1}$$

where $q > 0$ is a prescribed (temperature and material dependent) quantity. The latter condition fails near the transition temperature to nematic as \mathbf{n} experiences significant fluctuations with respect to the layer normal $\nabla\phi$.

We are interested in finding equilibrium configurations of $E(\Psi, \mathbf{n})$ subject to given boundary conditions, where

$$E = \int_{\Omega} L(|\nabla\Psi - iq\mathbf{n}\Psi|^2) + \mathcal{F}_A(|\Psi|) + \mathcal{F}_N(\nabla\mathbf{n}) \, d\mathbf{x} \tag{2}$$

In the previous expression, $\mathcal{F}_N(\nabla\mathbf{n})$ and $\mathcal{F}_A(|\Psi|)$ denote the nematic Oseen–Frank free energy and the smectic free energy, respectively. Since

$$|\nabla\Psi - iq\mathbf{n}\Psi|^2 = |\nabla\rho|^2 + \rho^2|\nabla\phi - q\mathbf{n}|^2 \tag{3}$$

fluctuations of the layer normal, $\nabla\phi$, with respect to the director \mathbf{n} as well as non-homogeneous distributions of the density, ρ , turn out to be energetically penalized. The contribution $\mathcal{F}_A(|\Psi|)$ favours special constant values of ρ , corresponding to equilibrium nematic or smectic A regimes. In particular, configurations with $\rho = 0$ represent the nematic phase, with the isotropic appearing as a special case of the nematic. The Oseen–Frank energy which penalizes changes in \mathbf{n} is given by

$$\begin{aligned} \mathcal{F}_N(\nabla\mathbf{n}) &= K_1(\nabla \cdot \mathbf{n})^2 + K_2(\mathbf{n} \cdot \nabla \times \mathbf{n})^2 + K_3(\mathbf{n} \times \nabla \times \mathbf{n})^2 \\ &\quad + (K_4 + K_2)(\text{tr}(\nabla\mathbf{n})^2 - (\nabla \cdot \mathbf{n})^2) \end{aligned} \tag{4}$$

The coefficients of the previous equation are material constants which may depend on the temperature. Moreover, the last term depends completely on the boundary values of \mathbf{n} , as a result of the identity,

$$\text{tr}(\nabla\mathbf{n})^2 - (\text{div}\mathbf{n})^2 = \text{div}((\nabla\mathbf{n})\mathbf{n} - (\text{div}\mathbf{n})\mathbf{n}) \tag{5}$$

As customary in many analyses involving the Frank–Oseen free energy, we consider the case where $K_1 = K_2 = K_3$. In this situation, \mathcal{F}_N becomes $\hat{K}(\nabla\mathbf{n})^2$ plus the boundary term. It is important to point out, though, that by making such a hypothesis, one neglects the fact

that the constant K_2 may grow very large near the temperature of transition to the smectic A phase [13].

The smectic A free energy, $\mathcal{F}_A(|\Psi|)$, is assumed to be smooth and it may exhibit one or more potential wells for the nematic and smectic A equilibrium states. Specifically, it is a polynomial in ρ which vanishes at zero. For example, it can have the following form:

$$\mathcal{F}_A(\rho) = a_1\rho^2 + a_2\rho^4 + a_3\rho^6, \quad a_1 \geq 0, \quad a_3 \geq 0 \quad (6)$$

Further constraints on a_i are discussed in Reference [12]. They are connected with first- and second-order phase transitions.

The scalar quantities q, L, a_1 , and \hat{K} represent the physical parameters of the problem. Letting $R > 0$ denote a typical length scale of the system, the dimensionless versions of the parameters are

$$\mu^{-2} = \frac{a_1 R^2}{L}, \quad \alpha = qR, \quad K = \frac{\hat{K}R}{a_1} \quad (7)$$

From now on, α denotes the dimensionless wave number of the smectic phase. We expect $0 < L \ll 1$ near the transition temperature to nematic, whereas $L \gg 1$ within the smectic A regime.

The present model allows for a characterization of the different types of defects that one may encounter. In the following sections, such defects will be discussed as special solutions of the equations. The set of points in Ω such that $\rho = 0$ represents a nematic defect. If $\rho \neq 0$, then defects are said to be of smectic type. Since \mathbf{n} describes the optical properties of the liquid crystal sample, defects that involve discontinuities in \mathbf{n} will be visible. Discontinuities in ϕ may not be visible.

- (1) A *disclination* is the set of points where \mathbf{n} and $\nabla\phi$ are discontinuous but ϕ is continuous. (When $\rho \equiv 0$, this reduces to the standard definition of disclination in nematics.)
- (2) A *dislocation* is the set of points where ϕ is discontinuous. Thus, $\nabla\phi$ has a singularity which is either removable or essential. If the singularity is removable then \mathbf{n} will be continuous. If the singularity is essential, then \mathbf{n} will also have a discontinuity, in which case the defect is also a disclination.

In order to describe non-polar liquid crystals the model must be invariant under the transformation $\Psi \rightarrow \Psi^*$. Invariance under this transformation guarantees that replacing \mathbf{n} by $-\mathbf{n}$ does not change the energy.

It is reasonable to argue that in the absence of external forces the material should be able to select the orientation \mathbf{n} or $-\mathbf{n}$ with equal energetic preference. We observe that the constraint term in (2) breaks the invariance of the energy with respect to the transformation of \mathbf{n} to $-\mathbf{n}$. This motivates the modification of (2) and to consider instead the following one:

$$E = \int_{\Omega} L |\nabla\Psi - iq\mathbf{n}\Psi|^2 |\nabla\Psi^* - iq\mathbf{n}\Psi^*|^2 + \mathcal{F}_A(|\Psi|) + \mathcal{F}_N(\nabla\mathbf{n}) \quad (8)$$

where $|\mathbf{n}| = 1$.

For the above energy, the reflection transformation of \mathbf{n} is equivalent to the complex dual transformation of Ψ .

These are two different energy formulations for the smectic A behaviour. The first is physically appropriate for modelling polar smectics. The non-polar energy satisfies the director

invariance, and therefore the second may be suitable for modelling regular smectic A phases. Both of these types have been discussed before. See Reference [12] and the references contained therein.

In Reference [14], Lubensky and Renn proposed an energy expression for the smectic A phase that involves fourth powers of (second)-order spatial gradients of Ψ . The purpose of such terms was to describe a ring in the X-ray scattering intensity above the nematic–smectic C transition. Whereas such a constraint also satisfies the invariant requirements for non-polar materials, the form (8) that we propose avoids the mathematical complications of dealing with second-order derivatives in the energy, at the expense, though, of omitting some effects that may be relevant near the smectic C transition.

3. EULER–LAGRANGE EQUATIONS AND SPECIAL SOLUTIONS

3.1. Polar smectic A energy

We let the liquid crystal occupy the domain Ω and consider the dimensionless version of the energy functional stated in (2) with the coefficients given in (7),

$$E = \int_{\Omega} \mu^2 (|\nabla \rho|^2 + \rho^2 |\nabla \phi - \alpha \mathbf{n}|^2) + \mathcal{F}_A(\rho) + \mathcal{F}_N(\nabla \mathbf{n}) \, d\mathbf{x} \tag{9}$$

Both smectic A and nematic phases can be treated within this model by allowing different limits in μ . In fact, as $\mu \rightarrow \infty$, minimizers of (9) must satisfy the condition, $\nabla \phi = \alpha \mathbf{n}$, and, consequently, $\nabla \times \mathbf{n} = 0$. (The former becomes $\phi' = \alpha$ for one dimensional geometries.) This is the case when the first term in (2) becomes the dominant one, with fluctuations from the purely smectic A regime resulting in large energy penalties. On the other hand if $\mu \rightarrow 0$, the term multiplying μ^2 can be regarded as playing a relaxation role in the energy, allowing for significant departures from the smectic A phase. This issue is addressed in Reference [12] in the study of the phase transition to nematic.

The Euler–Lagrange equation for ρ is given by

$$-\mu^2 \Delta \rho + \mu^2 \rho |\nabla \phi - \alpha \mathbf{n}|^2 + \frac{1}{2} \frac{d\mathcal{F}_A'(\rho)}{d\rho}(\rho) = 0 \tag{10}$$

The equation for ϕ is

$$\nabla \cdot (\rho^2 (\nabla \phi - \alpha \mathbf{n})) = 0 \tag{11}$$

Finally, the equation for \mathbf{n} is

$$\Delta \mathbf{n} - \alpha \rho^2 (\nabla \phi - \alpha \mathbf{n}) + \lambda \mathbf{n} = 0 \tag{12}$$

where λ is the Lagrange multiplier associated with the constraint $|\mathbf{n}| = 1$,

$$\lambda = |\nabla \mathbf{n}|^2 - \alpha \rho^2 (\nabla \phi \cdot \mathbf{n} - \alpha) \tag{13}$$

In this subsection, we let Ω be the region between two parallel plates, i.e.

$$\Omega = \{\mathbf{r} = (x, y, z): -1 < z < 1, \quad (x, y) \in \mathbb{R}^2\} \quad (14)$$

and assume that all quantities depend on z only. Then Equations (10)–(13) reduce to a system of non-linear ordinary differential equations with respect to $z \in (-1, 1)$:

$$-\mu^2 \rho'' + \mu^2 \rho |\phi' \mathbf{k} - \alpha \mathbf{n}|^2 + \frac{1}{2} \frac{d\mathcal{F}_A}{d\rho}(\rho) = 0 \quad (15)$$

$$(\rho^2(\phi' - \alpha \mathbf{k} \cdot \mathbf{n}))' = 0 \quad (16)$$

$$-\mathbf{n}'' - \alpha \rho^2 (\phi' \mathbf{k} - \alpha \mathbf{n}) + \lambda \mathbf{n} = 0 \quad (17)$$

Here *prime* denotes derivative with respect to z and \mathbf{k} is the unit vector along the z -direction. Weak solutions of (15)–(17) exist as a result of the ellipticity of the system. We now give a sample of special weak solutions in order to illustrate different types of singularities. (Such solutions satisfy the governing equations almost everywhere.)

(A1) The boundary conditions for the first special solution are

$$\rho(-1) = a, \quad \rho(1) = b, \quad \phi(-1) = A, \quad \phi(1) = B \quad (18)$$

$$\mathbf{n}(-1) = \mathbf{k} = \mathbf{n}(1) \quad (19)$$

where a, b, A and B are constants satisfying $B - A > 0$. The conditions on \mathbf{n} may be viewed either as corresponding to strong anchoring of the director in the bounding plates or as the result of wetting the surface. In the case that

$$a = 0 = b \quad (20)$$

one solution is $\rho \equiv 0$, ϕ is undefined (arbitrary) and \mathbf{n} satisfies the nematic equation from the Oseen–Frank energy.

Moreover in the case that $a_2 = 0 = a_3$ in (6), the maximum principle applied to smooth solutions of (15) indicates that $\rho \equiv 0$ is the unique solution for the boundary conditions (20). This is the nematic configuration. This special choice of coefficients corresponds to the case that the model contains only the purely nematic phase. However uniqueness of the nematic solution $\mathbf{n} = \mathbf{k}$ cannot be guaranteed. This is because (9) does not contain ‘surface energy’ to penalize defects consisting of \mathbf{n} changing to $-\mathbf{n}$. These special solutions do not admit any smectic defects. All the defects are nematic. Such type of solutions are also predicted by several other models of nematics (e.g. relaxed Ginzburg–Landau [15], Landau–de Gennes [16], Ericksen [17]). Such models often differ in the prediction of the defect structure in the interior of the sample.

(A2) Consider the same boundary conditions as in the first special solution where ρ is non-trivial on the boundary. In this case, letting

$$\mathbf{n} \equiv \mathbf{k}, \quad \phi' = \alpha \quad (21)$$

and ρ be the solution of

$$-\mu^2 \rho'' + \frac{1}{2} \frac{d\mathcal{F}_A}{d\rho}(\rho) = 0 \tag{22}$$

with boundary conditions as in (18) gives another special solution. This corresponds to a purely smectic A configuration. In particular, if $(d\mathcal{F}_A/d\rho)(r_1) = 0$ and $a = b = r_1$ in (18) then a solution of (22) for ρ is $\rho = r_1$. Depending on the value of $B - A$, there will be different ways for ϕ to satisfy the boundary conditions (18) and Equation (16).

Case 1: Suppose that $B - A = 2\alpha$. Then $\phi(z) = A + \alpha z$. This is the defect-free smectic configuration.

Case 2: Suppose that $B - A \neq 2\alpha$. Then a solution is such that one or more jumps in ϕ occur at points in the sample. However, the right and left limits of the derivative at such points are equal.

$$\sum_{1 \leq i \leq N} [\phi]_i = B - A - 2\alpha \tag{23}$$

where N denotes the number of jumps. In this configuration, all of the defects are dislocations.

(A3) A third type of special solution can only be obtained for *polar* smectic A material. While keeping the same boundary conditions as in the two previous special solutions for ρ and ϕ , replace those in (19) with the following:

$$\mathbf{n}(-1) = -\mathbf{k} \quad \text{and} \quad \mathbf{n}(1) = \mathbf{k} \tag{24}$$

The solution is

$$(\mathbf{n}, \phi) = \begin{cases} (-\mathbf{k}, A - \alpha(z + 1)) & \text{if } -1 < z < z_0 \\ (\mathbf{k}, B + \alpha(z - 1)) & \text{if } z_0 < z < 1 \end{cases} \tag{25}$$

with

$$z_0 = \frac{A - B}{2\alpha} \tag{26}$$

This solution presents a disclination, i.e. ϕ is continuous and ϕ' is discontinuous, taking values $\pm \alpha$, respectively, across z_0 . This is a visible defect since \mathbf{n} is discontinuous.

3.2. Non-polar smectic A

A simple calculation shows that the first term in the integrand of functional (8) involves the following terms:

$$\begin{aligned} |\nabla \Psi - i q \mathbf{n} \Psi|^2 |\nabla \Psi^* - i q \mathbf{n} \Psi^*|^2 &= |\nabla \rho|^4 + \rho^4 |\nabla \phi - q \mathbf{n}|^2 |\nabla \phi + q \mathbf{n}|^2 \\ &\quad + \rho^2 |\nabla \rho|^2 (|\nabla \phi - q \mathbf{n}|^2 + |\nabla \phi + q \mathbf{n}|^2) \\ &= |\nabla \rho|^4 + \rho^4 |\nabla \phi - q \mathbf{n}|^2 |\nabla \phi + q \mathbf{n}|^2 + 2\rho^2 |\nabla \rho|^2 (|\nabla \phi|^2 + q^2) \end{aligned} \tag{27}$$

Let the liquid crystal occupy the domain $\Omega \subset \mathbb{R}^3$. The dimensionless version of the energy functional stated in (8), with coefficients given in (7), and employing the relation (27) yields

$$E = \int_{\Omega} \mu^2 (|\nabla \rho|^4 + \rho^4 |\nabla \phi - \alpha \mathbf{n}|^2 |\nabla \phi + \alpha \mathbf{n}|^2 + 2\rho^2 |\nabla \rho|^2 (|\nabla \phi|^2 + \alpha^2)) + \mathcal{F}_A(\rho) + \mathcal{F}_N(\nabla \mathbf{n}) \, d\mathbf{x} \quad (9')$$

The corresponding Euler–Lagrange equations are derived in Reference [12] using the fact that $|\mathbf{n}| = 1$. The corresponding equations for ρ and ϕ are

$$\mu^2 (-2\chi_1 \rho \mathbf{n} \cdot \nabla \phi - \nabla \cdot (\chi_2 \nabla \rho) + \rho \chi_2 |\nabla \phi|^2 + \alpha^2 \chi_2 \rho) + \frac{1}{4} \frac{d\mathcal{F}_A}{d\rho} = 0 \quad (28)$$

$$\nabla \cdot (\chi_1 \rho \mathbf{n}) + \chi_1 \nabla \rho \cdot \mathbf{n} - (\nabla \cdot (\rho \nabla \phi \chi_2) + \chi_2 \nabla \phi \cdot \nabla \rho) = 0 \quad (29)$$

with

$$\chi_1 \equiv 2\alpha^2 \rho^2 \mathbf{n} \cdot \nabla \phi, \quad \chi_2 \equiv |\nabla \rho|^2 + \rho^2 |\nabla \phi|^2 + \alpha^2 \rho^2 \quad (30)$$

Formally, these Euler–Lagrange equations can be reduced to those in (10)–(12) if we set $\chi_1 = \alpha$ and $\chi_2 = 1$. This choice of χ_1 and χ_2 will hold if ρ is constant and \mathbf{n} is parallel to $\nabla \phi$. In this case the original non-polar energy reduces to the polar one.

In general, the non-linearity χ_2 becomes relevant when dealing with solutions such that second-order derivatives of Ψ become infinite at some points of the domain (e.g. the case when first gradients experience discontinuities). Since we expect ρ to become zero in such singular points, Equations (28)–(30) may admit solutions such that $\nabla \Psi$ becomes infinite there. Such types of non-linear structure do not appear in the case of the simpler constraint.

We now take \mathcal{F}_N as in (4) with equal coefficients in which case the Euler–Lagrange equation for \mathbf{n} is

$$-\Delta \mathbf{n} - 4\mu^2 \alpha^2 \rho^4 (\mathbf{n} \cdot \nabla \phi) \nabla \phi + \lambda \mathbf{n} = 0 \quad (31)$$

where

$$\lambda = -|\nabla \mathbf{n}|^2 + 4\mu^2 \alpha^2 \rho^2 (\nabla \phi \cdot \mathbf{n})^2 \quad (32)$$

As in the polar case, we now consider the one-dimensional configurations in the domain (14). In this case the Euler–Lagrange equations reduce to a system of non-linear ordinary differential equations with respect to $z \in (-1, 1)$:

$$\mu^2 (-2\chi_1 \rho \mathbf{n} \cdot \phi' \mathbf{k} - (\chi_2 \rho')' + \rho \chi_2 (\phi')^2 + \alpha^2 \chi_2 \rho) + \frac{1}{2} \frac{d\mathcal{F}_A}{d\rho}(\rho) = 0 \quad (33)$$

$$(\chi_1 \rho \mathbf{n} \cdot \mathbf{k})' + \chi_1 \rho' \mathbf{k} \cdot \mathbf{n} - ((\rho \chi_2 \phi')' + \chi_2 \phi' \rho') = 0 \quad (34)$$

$$-\mathbf{n}'' - 4\mu^2 \alpha^2 \rho^4 (\mathbf{n} \cdot \phi' \mathbf{k}) \phi' \mathbf{k} = |\mathbf{n}'|^2 - 4\mu^2 \alpha^2 \rho^2 (\mathbf{n} \cdot \phi' \mathbf{k})^2 \quad (35)$$

$$\chi_1 = 2\alpha^2 \rho^2 \phi' \mathbf{k} \cdot \mathbf{n}, \quad \chi_2 = \rho'^2 + \rho^2 (\phi')^2 + \alpha^2 \rho^2 |\mathbf{n}|^2 \quad (36)$$

We now consider special solutions for the non-polar energy. In such case one can find new solutions which do not have an analog in the polar case. This is due to the invariance of the energy under the transformation of \mathbf{n} to $-\mathbf{n}$ which motivated the non-convexity with respect to $\nabla\Psi$ in (8). We use the same boundary conditions for ρ and ϕ as in (18), and assign new ones to \mathbf{n} ,

$$\mathbf{n}(-1)=\mathbf{k} \quad \text{and} \quad \mathbf{n}(1)=\mathbf{k}$$

We look for solutions of the governing equations and point out different types of defects. Integrating Equation (34) yields

$$\rho^2|\phi'(2\alpha^2\rho^2n_3 - (\rho')^2 - \rho^2(\phi')^2 - \alpha^2\rho^2)|=K \tag{37}$$

where the parameter K is to be determined.

(B1) The first special solution is

$$\rho=0 \tag{38}$$

just as the corresponding one in the polar case. Since this represents the purely nematic phase there is no difference between the polar and non-polar solutions.

(B2) This solution is exactly as in the polar case. The defects are invisible dislocations as well.

(B3) This corresponds to the third special solution in the polar case, and with fields:

$$(\mathbf{n}, \phi) = \begin{cases} (\mathbf{k}, A - \alpha(z + 1)) & \text{if } -1 < z < z_0 \\ (\mathbf{k}, B + \alpha(z - 1)) & \text{if } z_0 < z < 1 \end{cases} \tag{39}$$

$$z_0 = \frac{A - B}{2\alpha} \tag{40}$$

This solution is such that ϕ is continuous and ϕ' is discontinuous, taking values $\pm\alpha$, respectively, across z_0 . Since \mathbf{n} is continuous, such defect may be labelled as a disclination which is not visible. Unlike the corresponding case of polar smectics, one remarkable feature of such a solution is that the director field is constant. This is the reason why such an example shows exactly the property of reflection invariance of the energy. Moreover, in contrast with the solution (B2), if only one defect is permitted in the present configuration, then the location of that defect is uniquely determined by the boundary data.

4. STABILITY OF THE FOCAL DOMAIN INTERFACE

In this section we study several types of two-dimensional focal conic pattern according to the mathematical features of the interfaces. One of the main ingredients of our analysis is the stability condition derived by Kinderlehrer and Liu [6], i.e.

$$\mathbf{n}_1 \cdot \nu = \pm \mathbf{n}_2 \cdot \nu \tag{41}$$

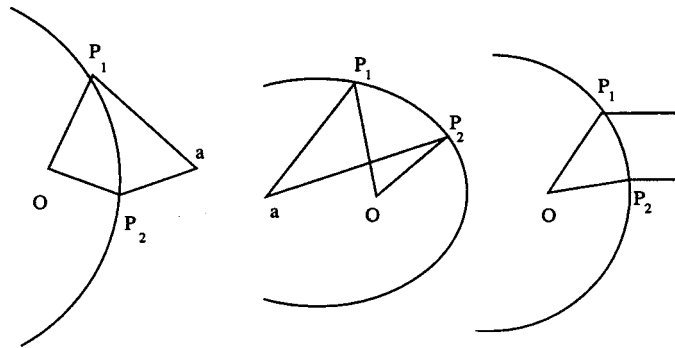


Figure 1.

where the \mathbf{n}_i , $i=1,2$, denote the director configurations on both sides of the interface, Γ , respectively, and ν denotes the normal to the curve. The stability condition is, in fact, the local version of the layer matching property. Specifically, the layer matching requirement establishes that the layers must be equidistant on both sides of the interface. This condition is also a local characterization of conic sections (quadratic curves).

In the case that Γ is a hyperbola, the solution on the one side preserves the concentric circular layers with the original centre, O , as shown in Figure 1. On the other side of Γ the solution consists of concentric layers as well, but with centre at the point a . The points O and a are two foci of the hyperbola interface. On both sides of the hyperbola both sets of fields are radially symmetric with respect to the corresponding centres.

The configurations with elliptic interface are the subject of our previous article [7]. There, we showed that given a radially symmetric, energy minimizing configuration $(\phi, \rho, \mathbf{n}_i)$ with a degree 1 defect in the centre O of the disk, another configuration with the same energy can be obtained by means of the following construction. We select a point a inside the disk, other than the origin, and then consider an elliptic interface with foci O and a . Inside the ellipse, the new fields, $(\phi_1, \rho_1, \mathbf{n}_1)$, are obtained from the original ones (ϕ, ρ, \mathbf{n}) by reflection with respect to the perpendicular bisector of the segment through the points $a/2$ and O . Outside the ellipse, the fields remain unchanged.

A degenerate case of both the elliptic and hyperbolic interfaces is the parabolic one. If one of the foci, a , is located at infinity the interface will become parabolic. The level sets of ϕ corresponding to the focus at infinity will be straight lines and the ones corresponding to the other focus, O , will remain circles. These three types of interface are illustrated in Figure 1.

In all three cases, the configuration on the one side of the conic section can be viewed as the ‘mirror reflection’ of the solution on the other side of the interface. The assumption of layer matching determines the shape of the interface. Moreover the fields (ϕ, ρ, \mathbf{n}) are discontinuous across Γ .

From the above discussion, it is clear that equilibrium configurations, and even energy minimizers are non-unique. Specifically, the present model does not have the capability to single out a unique minimizer. For this, it is necessary to include in the model a surface energy contribution associated with the interface. Such a procedure is illustrated in the next section for a wedge-shaped domain.

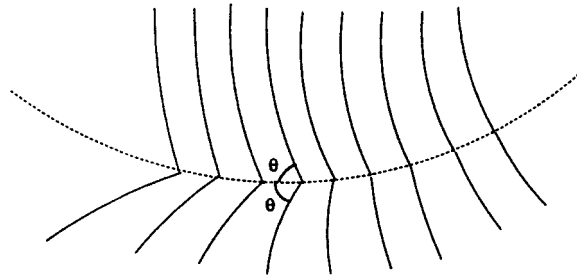


Figure 2.

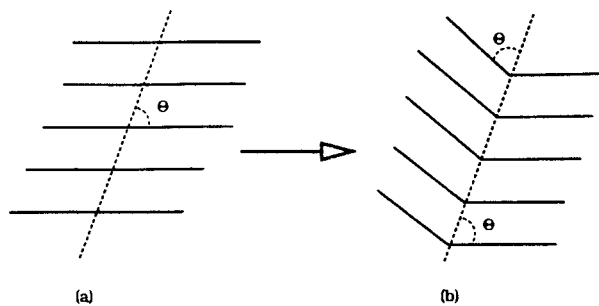


Figure 3.

One relevant fact in the study of smectic A solutions is that any energy minimizing configuration in two dimensions must have the level sets of ϕ in the shape of circles or lines. This follows from arguments in References [6, 7].

Finally, we point out that the construction of fields as discussed in Sections 3 and 4 provides weak solutions to the Euler–Lagrange equations. Such weak solutions can also be interpreted as limits of smooth solutions of the equations. For such smooth solutions, ρ vanishes at the interface as $\mu \rightarrow \infty$ (this corresponds to departure from the nematic regime). An illustration of a similar phenomenon can be found in Reference [12] in the case that $\mu \rightarrow 0$, i.e. for temperatures near the transition to nematic.

5. SMECTIC A CONFIGURATION IN A WEDGE DOMAIN

In this section we study focal conic configurations in wedge-type domains. For this, we first consider a focal conic structure with a hyperbolic interface in all of \mathcal{R}^2 as shown in Figure 2.

We subsequently allow the foci move further apart and tend to ∞ . At the limit, the hyperbola interface becomes a straight line and the circular layers become planar. Moreover, by the stability condition, the angles between the layers and the interface, on both sides of the domain, have the common value, Θ , as shown in Figure 3(b).

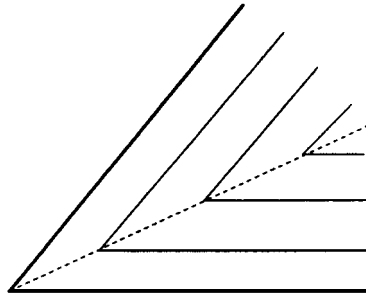


Figure 4.

An alternative way to carry out the construction of the previous configuration is the following. Starting with a planar parallel layer configuration in space (Figure 3(a)), we make a cut along a straight line at an angle Θ with the layers. We subsequently take the mirror reflection of the one half of the diagram with respect to the line and glue it back at the interface. It is easy to see that this construction does not alter the value of the total energy. (This is the plane layer argument analogous to the elliptic construction of the previous section.)

Next we consider the case that the boundary plates are non-parallel, that is, the domain is a wedge sustaining an angle equal to 2Λ (Figure 4). The boundary conditions on the new domain are

$$\mathbf{n} \parallel \nu \quad \text{and} \quad \nabla \phi = \alpha \nu \quad (42)$$

where ν is the outward normal vector to the domain boundary, and ρ is set to be a constant on each component of the boundary (as in Section 3). We now construct purely smectic solutions, i.e. the constraint $\nabla \phi = \alpha \mathbf{n}$ is identically satisfied. In such case, the non-linear elliptic equation for ρ does not involve \mathbf{n} and ϕ and, therefore it can be independently solved. To determine the layer structure of the solution, we consider an arbitrary line, L , that goes through the origin of the wedge. A layer configuration with layers parallel to the boundary in each subwedge satisfies the governing equations (11), (12) and boundary conditions (42) (see Figure 4). Finally, the stability condition (41) selects L as the bisector of the wedge into equal subwedges.

We point out that this configuration as well as the ones that follow share the property that the layer structures are determined in terms of the distance to the boundary. This results from the equal layer spacing condition together with the shape of the boundary as well as the nature of the boundary conditions.

The above construction is highly non-unique. In fact, it is not the only configuration satisfying the boundary conditions, the governing equations, and the stability condition (41). For instance, Figure 5 shows another possible solution consisting of two subwedges POC and COQ . The stability condition requires that for any ray OC , the line OA must bisect the wedge POC ; likewise, OB bisects COQ . This construction can be subsequently repeated at smaller and smaller scales to generate self-similar structures. Since the current model does not assign surface energy to defects (ellipse, hyperbola or line), there is no criteria to select a particular one among such configurations. Figure 4 corresponds to the case with the smallest number of defects.

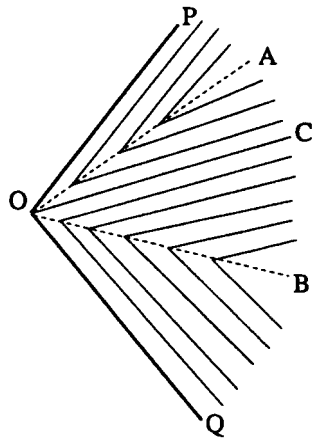


Figure 5.

Remark. There are many different forms for the surface energy and the particular choice will depend on the material properties of the individual sample. In particular, the distinction between the polar and non-polar nature of the liquid crystal will be taken into account. For instance, an interface energy for a polar material is

$$\int_{\Gamma} (1 - (\mathbf{n}^+ \cdot \mathbf{n}^-))^p dS \tag{43}$$

where Γ is the interface, \mathbf{n}^+ and \mathbf{n}^- are the directors on either side of the interface, respectively, S is the arc length parameter of the curve, and p is a positive number. For the wedge domain, if $p=1$, then all self-similar solutions have identical total energy. If $p > 1$, then the interface energy will tend to nucleate interfaces. If $p < 1$, then the optimal configuration is the one with the minimum number of interfaces. Moreover, a linear combination of the two types can be used to create an interface energy that selects a specific number of defects, for a given domain and boundary conditions. An energy which reflects the invariance present in the non-polar case is

$$\int_{\Gamma} (1 - |\mathbf{n}^+ \cdot \mathbf{n}^-|)^p dS \tag{44}$$

Studies of surface energy will appear in a forthcoming article.

The configuration presented in Figure 4 can also be viewed as a Chevron defect structure. To explain this, let us consider the intersection with the wedge bisector interface of two strips parallel to each side of the boundary, respectively. This wedge element has precisely the features of a Chevron configuration. On the other hand, if a strip parallel to the wedge does not meet with the interface, then such configuration may be labelled as tilted (cf. [18, 19, 5]).

The next example deals with a domain bounded by two non-parallel plates which do not meet at the vertex of the wedge but rather end at a plate perpendicular to the centre line L . The construction of the solution is based on decomposing the domain into two parallel strips plus a central wedge. Figure 6 represents the resulting configuration in the case that the container

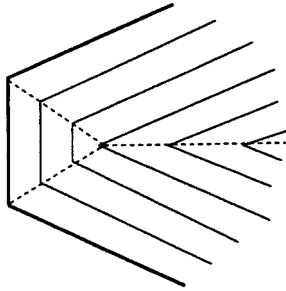


Figure 6.

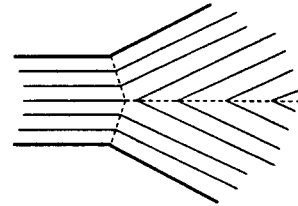


Figure 7.

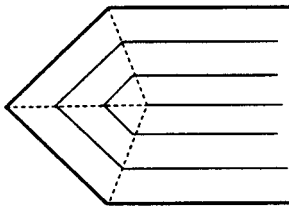


Figure 8.

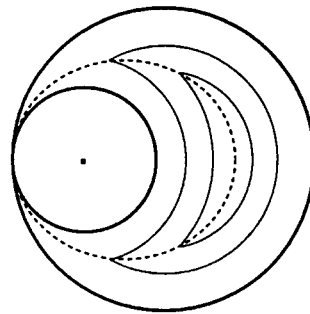


Figure 9.

is closed on the left side. We point out that there are three interfaces in the domain and each interface bisects the angle formed by two of the sides.

As a natural generalization, we consider the case that domain has the shape of a funnel. By combining both constructions, i.e. that of the case of parallel plates with that of the non-parallel ones, one can determine the solution completely. This is illustrated in Figure 7. On the other hand, in the case that a wedge ends in a strip, the construction of the solution is shown in Figure 8. As before, the interfaces bisect the angles made by the sides.

The case of concentric and non-concentric annular domains is also of interest. In such cases, one can also determine the singular interface across which solutions are discontinuous. The stability condition in this case will determine that the shape of the interface is an ellipse. The resulting configurations are illustrated in Figures 9 and 10. Of course in this case the special solution satisfies the Euler–Lagrange equation in the radial co-ordinate, as derived in Reference [7]. As in the case of the wedge, there are self-similar solutions for non-concentric annuli, with issues of non-uniqueness arising as well. One such configuration is shown in Figure 11. In this figure, C and D are the circular boundaries of the annulus and E and F are the focal defects (they are also elliptic). We emphasize that the layer configuration in this case is made up entirely of portions of circles.

Finally, we derive the layer configurations for convex as well as non-convex polygonal domains. The boundary conditions are analogous to those of the wedge domains. One special

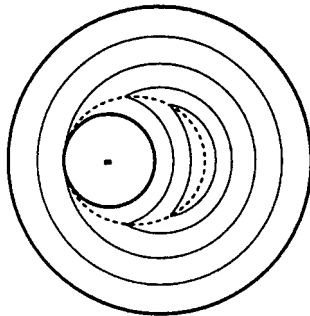


Figure 10.

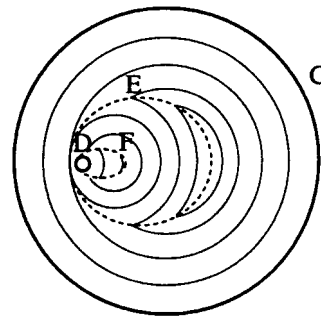


Figure 11.

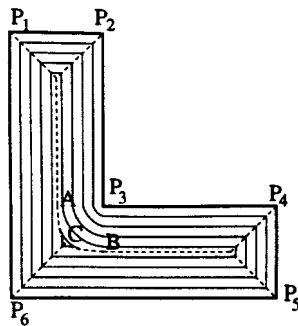


Figure 12.

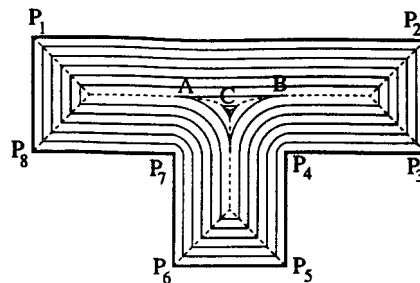


Figure 13.

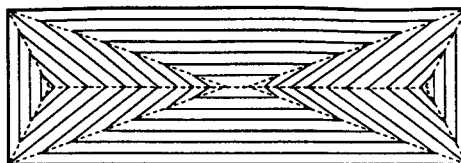


Figure 14.

feature encountered in the present case is that the interface for non-convex polygons may contain a piece of a parabola. For instance, in Figure 12, the interface AC is a parabola whose points are equidistant from the corner P_3 and the boundary segment P_1P_6 . The interface CB is also a parabola whose points are equidistant from P_3 and boundary segment P_5P_6 . The ends of the configuration are as in the wedge domains. In a more complex domain such as that in Figure 13, we also find a pair of parabolic interfaces. The first one is AC and these points are equidistant from P_7 and the boundary P_1P_2 . The second interface is BC with its points equidistant from P_4 and the boundary P_1P_2 . Finally, a self-similar solution for a rectangle is shown in Figure 14.

6. CONCLUSIONS

The study of smectic A configurations in a variety of geometrical settings illustrates the significant differences between nematic and smectic A behaviour. The layer spacing constraint of the latter results in very creative ways of material organization within a given domain. This, in turn, yields a very rich collection of pattern configurations that open up new interesting possibilities for display applications.

From a different point of view, studying solutions in several geometrical settings helps understanding the defect structures that naturally develop when even very small perturbations of the standard parallel plate and capillary shapes occur. This is again due to the difficulty of the smectic material to adapt to even very small changes that tend to disrupt the natural layer arrangements.

Finally, we point out that recent computer simulations carried out by Lai *et al.* [20] show an outstanding agreement with the configurations studied in this paper. We hope that future computational work will help in overcoming the mathematical difficulties of the three-dimensional modelling of focal conics.

ACKNOWLEDGEMENTS

M.C. Calderer has been supported by a grant from the National Science Foundation, contract no. DMS-9704714, 1997–1999.

REFERENCES

1. Friedel G. *Annals of Physics (Paris)* 1922; **2**:273–289.
2. Kleman M. Energetics of focal conics of smectic phase. *Journal Physique* 1977; **38**:1511–1524.
3. Boltenhagen P, Kleman M, Lavrentovich O. Focal conic domains in smectics. In *Soft Order in Physical Systems*, Rabin Y, Brumsma R, (eds.). Plenum Press: New York, 1994; 5–32.
4. Kralj S, Zumer S. Smectic A structures in submicrometer cylindrical cavities. *Physical Review E* 1996; **52**:1610–1617.
5. Ouchi Y, Takanishi Y, Takazoe H, Fukuda A. Chevron layer structures and parabolic focal conics in smectic-A liquid crystals. *Japanese Journal of Applied Physics* 1989; **28**:2547.
6. Kinderlehrer D, Liu C. Revisiting the focal conic structures in smectic A. *Proceeding Symposium on Elasticity to honor Professor J.L. Ericksen*. 1996.
7. Calderer MC, Liu C, Voss K. Radial configurations of smectic A materials and focal conics. *Physica D* 1998; **124**:11–22.
8. Weinan E, Garcia Cervera CJ. Dupin Cyclades. *Preprint*, 1996.
9. Stewart IW, Leslie FM, Nakagawa M. Smectic liquid crystals and the parabolic cyclides. *Quarterly Journal of Mechanics and Applied Mathematics* 1994; **47**:511–525.
10. Collings PJ, Patel J. *Handbook of Liquid Crystals*. Oxford University Press: Oxford, 1997.
11. De Gennes PG, Prost J. *The Physics of Liquid Crystals* (2nd edn.). Oxford University Press (Clarendon): London and New York, 1993.
12. Calderer MC, Palfy-Muhoray P. Ericksen's bar and modeling of the smectic A–nematic phase transition. *SIAM Journal on Applied Mathematics* 2000; **60**:1073–1098.
13. Takazoe H, Toyooka T, Horakata J, Fukuda A. Determination of twist elastic constant K_{22} by forced Rayleigh scattering. *Japanese Journal of Applied Physics* 1987; **26**:L240.
14. Lubensky W, Renn SR. Twist-grain-boundary phases near the nematic–smectic A–smectic C point in liquid crystals. *Physical Review A* 1990; **41**:4392–4401.
15. Bethuel F, Brezis H, Helein JM. *Ginzburg–Landau Vortices*. Birkhauser: Boston, Basel, Berlin, 1994.
16. Gartland C, Palfy-Muhoray P, Varga RS. Numerical minimization of the Landau-de Gennes free energy: defects in capillaries. *Molecular Crystals and Liquid Crystals* 1991; **199**:429–452.
17. Ericksen JL. Liquid crystals with variable degree of orientation. *Archives of Rational Mechanical Analysis* 1991; **113**:97–120.

18. Kralj S, Sluckin TJ. Landau-de Gennes theory of the Chevron structure in a smectic-A liquid crystal. *Physical Review E* 1994; **50**:2940.
19. Limat L, Prost J. A model for the Chevron structure obtained by cooling a smectic-A liquid crystal in a cell of finite thickness. *Liquid Crystals* 1993; **13**:101.
20. Lai MJ, Liu C, Wenston P. Theoretical and numerical analysis of two nonlinear biharmonic equations arising from the study of liquid crystals. *Preprint*, 1998.
21. Collings PJ. Phase structures and transitions in thermotropic liquid crystals. In *Handbook of Liquid Crystals*, Collings PJ, Patel JS (eds.). Oxford University Press: Oxford, 1997; 99–124.